Subject Specific Wall Shear Stress in the Human Thoracic Aorta

ROLAND GÅRDHAGEN
Linköping University
Department of Management and Engineering
581 83 Linköping
SWEDEN
roland.gardhagen@liu.se

JOHAN RENNER
Linköping University
Department of Management and Engineering
581 83 Linköping
SWEDEN
johan.renner@liu.se

TOSTE LÄNNE
Linköping University
Department of Medicine and Health Sciences
581 83 Linköping
SWEDEN
tosla@imv.liu.se

MATTS KARLSSON
Linköping University
Department of Management and Engineering
581 83 Linköping
SWEDEN
matts.karlsson@liu.se

Abstract: Numerous studies have shown a correlation between Wall Shear Stress (WSS) and atherosclerosis, but few have evaluated the reliability of estimation methods and measures used to assess WSS, which is the subject of this work. A subject specific vessel model of the aortic arch and thoracic aorta is created from MRI images and used for CFD simulations with MRI velocity measurements as inlet boundary condition. WSS is computed from the simulation results. Aortic WSS shows significant spatial as well as temporal variation during a cardiac cycle, which makes circumferential values very uninformative, and approximate estimates using Hagen-Poiseuille fails predict the average WSS. Highly asymmetric flow, especially in the arch, causes the spatial WSS variations.

Key–Words: Wall shear stress, CFD, Aorta, Circumferential average values, Asymmetric flow

1 Introduction

Wall Shear Stress (WSS), the frictional load from the blood on the vessel wall, and its role in the genesis and progression of atherosclerosis have been subject for numerous studies since the late 1960's [1, 2, 3, 4, 5]. It is believed to influence the function of the endothelial cells [6]; a functional endothelium is of crucial importance to maintain hemodynamic stability, and dysfunctional endothelial cells may for example enhance uptake of lipoproteins and leukocyte adhesion [7], thus promoting initiation of an atherosclerotic plaque. Several studies have found regions with low and/or oscillating WSS to be more prone to the development of disease [1, 3, 5]. Recent findings also suggest different properties of atherosclerotic lesions depending on whether WSS is low or oscillating [8]. Furthermore, if an atherosclerotic plaque ruptures or erosion injures the covering endothelial cell layer, a coagulation process initiates to heal the damaged wall. High shear stress now stimulates thrombosis at the site of the injury [9], and the growing thrombus may eventually occlude the entire vessel causing severe ischemic disease or infarction. Different levels of WSS may thus be dangerous during different stages of the disease. According to the definition, Eq. (1), WSS is obtained as the viscosity times the velocity gradient normal to the wall at the wall (wall shear rate, WSR).

$$\mathrm{WSS} = \mu \cdot \mathrm{WSR} = \mu \frac{\partial V}{\partial n}\Big|_{wall} \tag{1}$$

WSS is, however, frequently computed with Eq. (2) (or some equivalent equation) [10, 11, 12, 13, 14, 15, 16, 17]; the formula is derived for fully developed, stationary, laminar flow of a Newtonian fluid with constant viscosity, μ, in a straight, circular pipe with constant radius r, and provides a circumferential average in a cross section with volume flow rate Q. This particular flow is known as Hagen-Poiseuille flow [18, 19].

$$\mathrm{WSS}_{HP} = \frac{4\mu Q}{\pi r^3} \tag{2}$$

Difficulties to accurately and easily compute WSR have hampered a direct use of Eq. (1) for a long time, but with increased computer capacity and sophisticated numerical techniques it is now possible to compute a sufficiently detailed flow field, which gives the necessary WSR.

Limitations of WSS_{HP} have been addressed earlier [20] but the authors have not found any study contrasting circumferential average values in general with local, subject specific WSS. The aim of this work is to investigate the information contained in circumferential average values.

2 Method

Patient specific anatomy and flow data of a 23-year-old healthy male volunteer (184cm, 83kg) were acquired under resting conditions at the Center for Medical Image Science and Visualization (CMIV) [21] using a 1.5T MRI scanner (Philip's Achieva, Philips Medical Systems, Best, the Netherlands). Geometrical information of the aorta was extracted as sagittal images (in-plane resolution 0.78x0.78mm, slice thickness 1 mm) from a contrast enhanced magnetic resonance angiography and used to construct a geometrical model of the vessel Fig. 1 (Left).

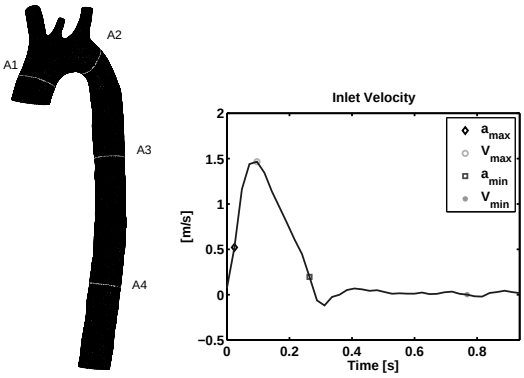

Figure 1: Left: Subject specific model of a human thoracic aorta. A1, A2, A3, and A4 are planes where WSS is studied. Right: Average inflow velocity during a hear beat.

The procedure followed a semi-automatic work flow described in [22]. In short, a fast level set segmentation located the inside of the vessel wall in the images resulting in a cloud of points approximating the luminal boundary. The points were smoothed using a 3D Gaussian smoothing filter of radius 2mm and thereafter joined by a surface mesh [23]. The computational mesh was constructed with ICEM 10.0 (ANSYS, Inc., Canonsburg, Pennsylvania, USA). It consisted of unstructured tetrahedral cells with a maximum size of 1.2mm. Five layers of prism elements were inserted at the wall to increase the resolution in this region. The volume of the vessel model was 67.7cm^3 and it contained about 1.04 million cells including the prism layers. To ensure reliable results, grid independence for the WSS [24] was verified by simulations with finer meshes where the maximum cell size was decreased to 1mm and 0.8mm without any effect on the WSS.

CFD simulations of the flow through the vessel were performed using Fluent 6.1.18 (Fluent Inc., Lebanon, New Hampshire, USA). Fluent uses a finite volume method to solve the Navier-Stokes' equations that govern the flow. Neglecting body forces, these equations can be written as

$$\nabla \cdot \mathbf{V} = 0 \tag{3}$$

$$\frac{\partial(\rho \mathbf{V})}{\partial t} + \nabla \cdot (\rho \mathbf{V}\mathbf{V}) = -\nabla p + \nabla \cdot \boldsymbol{\tau} \tag{4}$$

where $\boldsymbol{V}$ is the velocity vector, p the pressure, ρ the density, and $\boldsymbol{\tau}$ the stress tensor with components determined as

$$\tau_{ij} = \mu \left(\frac{\partial u_i}{\partial x_j} + \frac{\partial u_j}{\partial x_i} \right) \tag{5}$$

The fluid was assumed incompressible, with density 1060kg/m^3, and Newtonian, with dynamic viscosity μ=0.00345Ns/m^2. All simulations were performed at National Supercomputer Center [25], on the 400-CPU Linux cluster Monolith.

Time resolved velocity distribution at the model inlet (in the ascending aorta) was measured by a through-plane 2D velocity MRI acquisition (in-plane resolution 1.73x1.73mm, slice thickness 10mm), also described in [22], and used as inlet boundary condition. 40 time frames covering one heart beat of 0.92s were extracted from the measurements and corresponded to a time step of about 0.024s. To avoid numerical instability the number of time frames was doubled (using linear interpolation), reducing the time step size to 0.012s. Fig. 1 (Right) shows the average velocity normal to the inlet boundary during a heart beat.

The measured velocity distribution does in no way form a fully developed profile, but showed large spatial and temporal variations. For this reason, a second simulation with the same mass flow rate, but with a fully developed laminar velocity profile at the inlet, was run for comparison. Rigid walls were assumed together with a no-slip boundary condition; at the outflows the boundary condition ensured conservation of mass, and specified the fraction of fluid leaving each outlet: 10% in the brachiosephalic trunk, 5% in each of the left common carotid artery and the left subclavian artery, while 80% of the fluid continued to the abdominal part. During the first simulated cardiac cycle, especially before peak systole, WSS was affected by the initial condition of zero velocity in the

entire computational domain, while no significant differences were found between the second and third cycle; all values for the analysis were taken from the second cardiac cycle. Four cross sections were selected for the analyses, and they were denoted A1, A2, A3, and A4, respectively, see Fig. 1 (Left). A1, A2, and A3 were chosen in accordance with suggestions in [26] (A1: aortic arch entrance, A2: mid aortic arch, and A3: descending aorta). Plane A4 was chosen as a location where the flow might show best resemblance to Hagen-Poiseuille flow. To assess WSS_{HP} as a measure of the circumferential average WSS a corresponding value denoted WSS_{av} was computed as the average of WSS in all cells on the circumference of a cross section. Both WSS_{av} and WSS_{HP} are computed at every time step. The volume flow rate required for WSS_{HP} was obtained as the mass flow rate divided by the density. Since the aortic cross section is not perfectly circular, there is no trivial choice of radius, r, of a cross section. To obtain a reasonable estimate we applied an approach described in [16], where the radius r of a (non-circular) cross section with area A is taken as the radius of a circle with area A ($r_{A1} = 10.6$mm, $r_{A2} = 8.7$mm, $r_{A3} = 8.8$mm, and $r_{A4} = 9.3$mm). Four time points were chosen for the analysis: maximum acceleration (a_{max}), maximum velocity (V_{max}), minimum acceleration (maximum deceleration) (a_{min}), and minimum velocity (lowest magnitude) (V_{min}), see Fig. 1 (Right). a_{max}, V_{max}, and a_{min} were chosen in accordance with [26].

3 Result and Discussion

As a vector quantity WSS has a magnitude as well as a direction. Both of these properties are shown to be of crucial importance for the genesis and pathogenesis of atherosclerosis, as low magnitude and frequent changes of direction are correlated with increased intima media thickness [3, 4, 5], an early stage of atherosclerosis. In several studies WSS is assessed by means of circumferential average values of the magnitude [10, 11, 12, 13, 14, 15, 16, 17], and in this work we have investigated the information contained in such values. This was done using a subject specific model of a human aorta with a physiologic flow based on time resolved velocity measurements, which served as inlet boundary condition in the ascending aorta.

An atherosclerotic lesion will affect the flow significantly wherever it occurs; it acts as a throttling causing increased pressure (and work for the hart) distally and lowered pressure in proximal vessels. Apart from this clinical aspect plane A1 to A4 are relevant for the study as they represent different positions of a developing flow.

WSS_{HP}, often used as a measure of circumferential average WSS, in A1, A2, A3, and A4 is shown in Fig. 2 (Upper) and corresponding values of WSS_{av} are seen in Fig. 2 (Lower). Both measures show largest values during systole (0-0.3s), as expected, since this is when the blood is pumped into the aorta, and hence the velocity is high with large gradients at the wall. WSS_{HP} is, however, much lower than WSS_{av} in all the studied cross sections during the entire pulse, and does not predict the relative order between the planes. WSS_{HP} is almost identical in A2 and A3 since volume flow rates and area are equal, while the slightly larger area of A4 causes its lower WSS_{HP}. Maximum difference ($\mathrm{WSS}_{av} \approx 13 \cdot \mathrm{WSS}_{HP}$) and minimum difference ($\mathrm{WSS}_{av} \approx 5 \cdot \mathrm{WSS}_{HP}$) are found in A2 and A4, respectively.

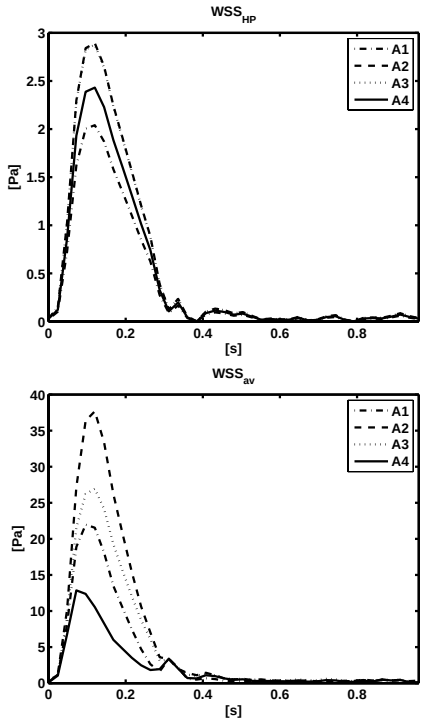

Figure 2: Upper: WSS_{HP} in A1, A2, A3, and A4 during a cardiac cycle. Lower: WSS_{av} in A1, A2, A3, and A4 during a cardiac cycle.

Systole lasts approximately one third of the cardiac cycle, during which the endothelial cells are subjected to a relatively high WSS; during the rest of the pulse persisting motion still causes a WSS_{av} of almost 0.5Pa. However, since the net volume flow rate through any cross section is essentially zero after 0.3s, so is WSS_{HP}. This highlights a severe lack; low net volume flow rate might very well be the result of a partial flow reversal. A situation when WSS not only may be high, but also changes direction within the cross

section. WSS_{av} has a similar limitation and might be canceled if WSS changes direction within the cross section.

The reason to the total failure of WSS_{HP} to estimate the circumferential average WSS is found in Fig. 3 showing the velocity magnitude in A1, A2, A3, and A4 when the inflow velocity is maximal, i.e. at peak systole. In the ascending aorta the profile is rather blunt, but when passing through the arch it distorts to a skew profile with higher velocity on the inner side, Fig. 3 (Upper right). After the arch the high-velocity region moves toward the opposite side of the vessel and the highest velocity in A3 is found posterior. A fully developed flow would imply concentric circles, and something resembling that is only found in A4, where, accordingly, the difference betweenWSS_{av} and WSS_{HP} is smallest. The profile is, however, still more blunt than parabolic. Large velocity gradients at the wall otherwise cause much more friction than in the case of fully developed flow. The flow was assumed laminar, and studies of the Reynolds number indicated that it mostly was below the critical value of 2300, in addition, the transition in pulsatile flows has been shown to occur at even higher Reynolds numbers [27].

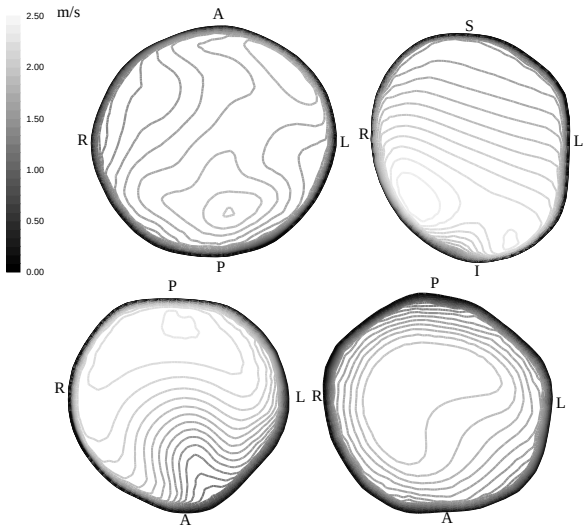

Figure 3: Velocity contours at V_{max} in A1 (Upper left), A2 (Upper right), A3 (Lower left), and A4 (Lower right). A: anterior, P: posterior, S: superior, I: inferior, L: left, R: right.

To assess WSS_{av} as a measure of WSS the latter was studied in detail and is shown in Fig. 4 (Upper left) A1, (Upper right) A2, (Lower left) A3, and (Lower right) A4. WSS is maximal at peak systole, i.e. at V_{max}, as is the spatial variation, a direct consequence of the complex flow field, and correlations between Fig. 3 and Fig. 4 are easy to find. The small region with low velocity inferior in A2 coincides with a minimum in Fig. 4 (Upper right), while high velocity in the right/posterior region of A3 causes a region of high WSS as seen in Fig. 4 (Lower left). The temporal variation was large in A1, A2, and A3 but more moderate in A4, which might indicate that the flow in the lower thoracic aorta is more developed and that recirculation and retrograde flow mainly exist near the arch. This is supported by Fig. 3 (Lower right), which shows very moderate circumferential velocity gradients in A4. Hence, the flow field itself does not solely cause the WSS fluctuations in Fig. 4 (Lower right), instead that variation is mainly caused by the geometry since the cross section is not perfectly circular. Neither is on the other hand A2 and A3, but the velocity field does apparently cause significantly greater changes of WSS, that dominate over geometry related variations. Thus, whereas the velocity field causes changes in WSS with as much as 40-50Pa, normal irregularities of the vessel wall only causes changes of about 5-10Pa under resting conditions.

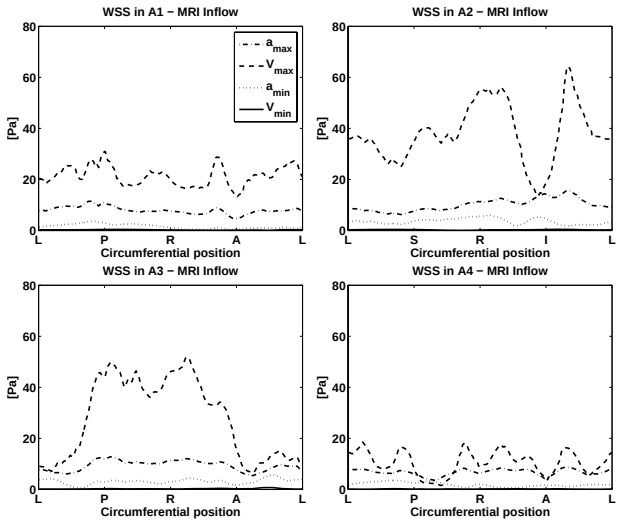

Figure 4: WSS in A2 when the inlet velocity is (Left) subject specific and (Right) fully developed laminar.

The influence of the inflow velocity profile was investigated by a simulation with equal mass flow rate entering the vessel but with the flow specified as fully developed laminar. Fig. 5 shows WSS in A2 (Left) and A3 (Right) at peak systole with a laminar velocity profile at the inlet. The inflow profile is seen to influence the flow and WSS in the arch whereas more distal flow appears to be unaffected. The spatial variation and average WSS in A2 were still high and consequently WSS_{HP} did not reasonably estimate WSS_{av} despite the favorable inflow profile. In fact, since the volume flow rate (mass flow rate divided by density) is the same, WSS_{HP} is identical in these two cases.

The adjustment of the flow indicates that each vessel ”forms” its own flow, which emphasizes the need for subject specific geometries, and therefore an accurate reconstruction of the vessel is of crucial importance.

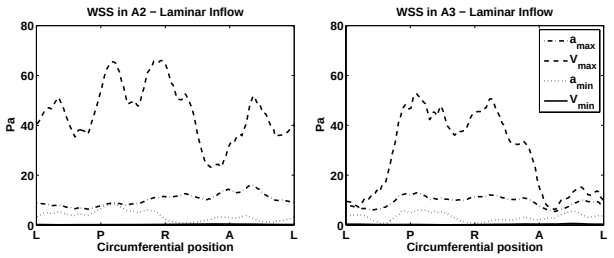

Figure 5: WSS in A3 when the inlet velocity is (Left) subject specific and (Right) fully developed laminar.

Since WSS changes this much even within a cross section, it is obvious that a circumferential average value offers limited information about the actual condition. This is important since the correlation with increased intima media thickness and atherosclerosis is the primary reason to the intense studies of WSS. The lesions are normally concentrated to one region of a cross section, see photos in e.g. [28] or [29], rather than being uniformly distributed around the circumference. Hence, the irregular aortic WSS pattern does probably influence the pathogenesis and should be evaluated locally, and not on cross sectional basis. This argues strongly against average values as a measure of aortic WSS, and idealized measures based on Hagen-Poiseuille or even Womersley flow should be avoided. Womersley flow does take pulsatile effects into account, but is still a model of an axisymmetric flow with constant WSS in the entire cross section.

Assumptions of Newtonian and laminar flow in a rigid vessel were made in the study, and the greatest violation of reality is probably the rigid walls since the aorta is an elastic artery. The Windkessel effect damps the pulsatility by buffering flow in the distal aorta during systole that continues during diastole. With Fig. 2 in mind it seems reasonable to expect systolic WSS to decrease and diastolic WSS to increase slightly. Blood flow is found to behave Newtonian for shear rates above $100s^{-1}$ and we have seen that this is the case except during parts of diastole, hence the largest differences are clearly not affected by this assumption and due to the limited time and regions where the shear rate is less than $100s^{-1}$ it seems reasonable to assume that the assumption of Newtonian flow does not harm the results.

4 Conclusion

We conclude that cross sectional average values like WSS_{av} are too vague measures of WSS in the human aorta, and yet more simplified approaches like WSS_{HP} do not estimate WSS accurately. Subject specific models are of crucial importance for correct estimation, as each vessel seems to form its own flow.

Acknowledgements: This work has been conducted in collaboration with the Center for Medical Image Science and Visualization (CMIV) at Linköping University, Sweden. CMIV is acknowledged for provision of financial support and access to leading edge research infrastructure.

References:

[1] DL. Fry, Acute vascular endothelial changes associated with increased blood velocity gradients, *Circ. Res.* 22, 1968, pp. 165-197

[2] CG. Caro, JM. Fitz-GeraldM and RC. Schroter, Atheroma and arterial wall shear. Observation, correlation and proposal of a shear dependent mass transfer mechanism for atherogenesis, *Proc. R. Soc. Lond. B. Biol. Sci.* 177, 1971, pp. 109-159.

[3] JE. Moore jr, C: Xu, S. Glagov, CK . Zarins and DN. Ku, Fluid wall shear stress measurements in a model of the human abdominal aorta: oscillatory behavior and relationship to atherosclerosis, *Atherosclerosis* 110, 1994, pp. 225-240.

[4] HM. Honda, T: Hsiai, CM. Wortham, M. Chen, H. Lin, M. Navab and LL. Demer, A complex flow pattern of low shear stress and flow reversal promotes monocyte binding to endothelial cells, *Atherosclerosis* 158, 2001, pp. 385-390.

[5] C: Irace, C. Cortese, E. Fiaschi, C. Carallo, E. Farinaro and A. Gnasso, Wall shear stress is associated with intima-media thickness and carotid atherosclerosis in subjects at low coronary heart disease risk, *Stroke* 35, 2004, pp. 464-468.

[6] MAJ. Gimbrone, N. Resnick, T. Nagel, TC. Khachigian and JN. Topper, Hemodynamics, Endothelial Gene Expression, and Atherogenesis. *Ann. NY. Acad. Sci.* 15, 1997, pp. 1-10

[7] O. Traub and BC. Berk, Laminar Shear stress, Mechanisms by Which Endothelial cells Transducean Atheroprotective Force, *Arter. Thromb. Vasc. Biol.* 5, 1998, pp. 677-685.

[8] C. Cheng, D. Tempel, R. van Haperen, A. van der Baan, F. Grosveld, MJ. Daemen, R. Krams

and R. de Crom R, Atherosclerotic lesion size and vulnerability are determined by patterns of fluid shear stress, *Circulation* 113, 2006, pp. 2744-2753.

[9] ER. Mohler III and AI. Schafer, Atherothrombosis: Disease Initiation, Progression, and Treatment, In *Williams Hematology*, 7th edition, Edited by Lichtman MA, EB, Kipps TJ, Seligsohn U, Kaushansky K, Prchal JT, Lewin RA, McGraw-Hill, 2006.

[10] R. Dammers, F. Stit, JHM. Tordoir, JMM. Hameleers, APG. Hoeks APG and PJEHM. Kitslaar, Shear stress depends on vascular territory: comparison between common carotid and brachial artery, *J. Appl. Physiol.* 94, 2003, pp. 485-489.

[11] JA. Ekaterinaris, CV. Ioannou and AN. Katsamouris, Flow Dynamicsin Expansions Characterizing Abdominal Aorta Aneurysms, *Ann. Vasc. Surg.* 20, 2006, pp. 351-359.

[12] FMA. Box, J. van der Grond, AJM. de Craen, IH. Palm-Meinders, RJ. van der Geest, GJ. Wouter Jukema, JHC. Reiber, MA. van Buchem and GJB. Blauw, Pravastatin Decreases Wall Shear Stress and Blood Velocity in the Internal Carotid Artery without Affecting Flow Volume. Results from the PROSPER MRI Study, *Stroke* 38, 2007, pp. 1374-1376.

[13] S. Misra, DA. Woodrum, J. Homburger, S. Elkouri, JN. Mandrekar,V. Barocas, JF. Glockner, DK. Rajan and D. Mukhopadhyay, Assessment of wall shear stress changes in arteries and veins of arteriovenous polytetrafluoroethylene grafts using magnetic resonance imaging. *Cardiovasc. Intervent. Radiol.* 29, 2006, pp. 624-629.

[14] GF. Mitchell, H. Parise, JA. Vita, MG. Larson, E. Warner, JF. Keaney Jr, MJ. Keyes, D. Levy, RS. Vasan and EJ. Benjamin, Local shear stress and brachial artery flow-mediated dilation: the Framingham Heart Study. *Hypertension* 44, 2004, pp. 134-139.

[15] DM. Wootton and DN. Ku, Fluid Mechanics of Vascular Systems, Diseases, and Thrombosis, *Annu. Rev. Biomed. Eng.* 1, 1999, pp. 299-329.

[16] A. Thury, G. van Langenhove, SG. Carlier, M. Albertal, K. Kozuma, E. Regar, G. Sianos, JJ. Wentzel, R. Krams, CJ. Slager, JJ. Piek and PW. Serruys PW, High shear stress after successful balloon angioplasty is associated with restenosis and target lesion revascularization, *Am. Heart. J.* 144, 2002, pp. 136-143.

[17] JN. Oshinski, JL. Curtinand F. Loth, Mean-average wall shear stress measurements in the common carotid artery. *J. Cardiovasc. Magn. Reson.* 8, 2006, pp. 717-722.

[18] DJ. Tritton DJ, *Physical Fluid Dynamics*, Clarendon Press, Oxford 1988.

[19] WW. Nichols and MF. O'Rourke, *McDonald's Blood Flow in Arteries*, Edward Arnold, London–Melbourne–Auckland 1990.

[20] D. Katritis, L. Kaiktsis, A. Chaniotis, J. Pantos and EP. Estathopoulos, Marmarelis V: Wall Shear Stress: Theoretical Considerations and Methods of Measurement, *Progress in Cardiovascular Diseases* 49, 2007, pp. 307-329.

[21] The Centre for Medical Image Science and Visualization (CMIV), http://www.cmiv.liu.se.

[22] J. Renner, R. Gårdhagen, E. Heiberg, T. Ebbers, D. Loyd, T. Länne T and M. Karlsson, Feasibility of Patient Specific Aortic Blood Flow CFD Simulation, In *Proceedings of Medical Image Computing and Computer-Assisted Intervention -MICCAI 2006*, October 2006, Copenhagen. Edited by Larsen R, Nielsen M, Sporring J, Stoneham, Butterworth-Heinemann 2006, pp. 257-263.

[23] E. Heiberg, *Automated Feature Detection in Multidimensional Images*, Dissertations No..917, PhD thesis, Linköping University, Depts.of Biomedical Engineering and Medicine and Care, Centre for Medical Image Science and Visualization, 2004.

[24] S. Prakash and CR. Ethier, Requirements for Mesh Resolution in 3D Computational Hemodynamics, *J. Biomech. Eng.* 123, 2001, pp. 134-144.

[25] National Super Computer Centre (NSC), http://www.nsc.liu.se.

[26] L. Morris, P. Delassus, A. Callanan, M. Walsh, F. Wallis, P. Grace and T. McGloughlin T, 3-D numerical simulation of blood flow through models of the human aorta, *J. Biomech. Eng.* 127, 2005, pp.767-775.

[27] YC. Fung, *Biomechanics: Motion, Flow, Stress, and Growth* Springer –Verlag, New York–Berlin–Heidelberg 1990

[28] C. Glass and JL. Witztum, Atherosclerosis: The Road Ahead, *Cell* 104, 2001, pp. 503-516.

[29] AJ. Lusis, Atherosclerosis, *Nature* 407, 2000, pp. 233-241.